ADVANCED OPTICAL MATERIALS
www.advopticalmat.de

High-Efficiency Photoluminescence Wholly Aromatic Triarylamine-based Polyimide Nanofiber with Aggregation-Induced Emission Enhancement

*Hung-Ju Yen, Jia-Hao Wu, Wen-Chang Wang, and Guey-Sheng Liou**

Novel AIE-active, high T_g (up to 420 °C), and solution-processable wholly aromatic polyimides with triarylamine chromophores are synthesized and fabricated into highly efficient photoluminescence (PL) nanofibers by an electrospinning method. The PL intensity of polymer solutions is induced by aggregation in poor solvents, and they could be fabricated into solid films with high PL quantum yields of up to 22%, demonstrating their aggregation-induced emission feature. Moreover, the electrospun nanofibers have the highest PL quantum yield of 26% among aromatic polyimides, suggesting their great potential for high-performance optoelectronic applications.

1. Introduction

The wholly aromatic polyimides (PIs) are well-known super engineering plastics exhibiting excellent thermal and chemical stability, flame resistance, radiation resistance, mechanical strength, and good flexibility.[1] Aromatic PIs synthesized from pyromellitic dianhydride and bis(4-aminophenyl)ether (PMDA/ODA) and from 3,3′,4,4′-biphenyltetracarboxylic dianhydride and *p*-phenylenediamine (*s*-BPDA/PDA) are representative ones, which have been commercialized as Kapton and Upilex-S, respectively. Aromatic PIs have been used in a wide range of high-tech fields, such as aerospace, electric, electronic and photonic applications.[2]

The optical absorption and fluorescence properties of aromatic PIs have been widely studied,[3] and reported that two kinds of UV/vis absorption bands are observed for wholly aromatic PIs.[3h] The first one is a locally excited (LE) transition that occurs between the occupied and unoccupied molecular orbitals (MOs), both of which are located around the dianhydride or diamine moieties. The second one is the charge transfer (CT) transition that is excited from MOs located around the diamine moiety to those around the dianhydride moiety. It is known that the CT transition is significantly influenced by the electron-donor diamine and the electron-acceptor dianhydride,[4] which has been commonly observed in wholly aromatic PIs.[5,3a–d]

Dr. H.-J. Yen, J.-H. Wu, W.-C. Wang, Prof. G.-S. Liou
Functional Polymeric Materials Laboratory
Institute of Polymer Science and Engineering
National Taiwan University
1 Roosevelt Road, 4th Sec., Taipei, 10617, Taiwan
E-mail: gsliou@ntu.edu.tw

DOI: 10.1002/adom.201300181

Hitherto, several aromatic PIs containing fluorescent moieties in the main chain or side chain have been synthesized and investigated.[6] However, these PIs could only reveal PL qauantum yield (Φ_{PL}) less than 15% because of the strong intermolecular CT and van der Waals interactions when fabricated into thin solid films, presenting an intractable problem of aggregation-caused quenching (ACQ).[7] Recently, some investigations reported that the utilization of the alicylic diamines or dianhydrides is an effective concept for preparing highly fluorescent PIs by preventing CT complex (CTC) formations.[8] However, in our knowledge, the wholly aromatic PIs with higher fluorescent Φ_{PL} in solid state have far not been successfully prepared, and still is a challenging and interesting project to be dealt with.

Therefore, the molecular design strategy is adopted in this report by the embedment of various fluorescent aggregation-induced emission (AIE) triarylamine moieties into the wholly aromatic PIs, and fabricates the polymeric nanofiber by electrospinning method, which was taken into account considering the following points: (1) The CT interactions would be efficiently decreased by the introduction of triarylamine unit as *N*-linked dianhydride into the polyimide backbone. (2) Structural modification of traditional luminophores by AIE groups may works as new effective way to transform ACQ luminophores to AIE luminogens. The propeller-like structure and electron-donating characteristic of triarylamine derivatives make it a useful building block for the construction of AIE luminogens, which is exactly the opposite of the ACQ effect, and paves a new avenue for the efficient solid-state applications.[8d,9] Moreover, recent studies have also depicted that the heteroatom-containing luminogens, siloles, luminogens with cyano substituents and hydrogen bonds all possess an excellent contribution in light emission.[9] (3) Electrospinning has emerged as a new technique recently to produce various functional nanofibers, producing more extended chain conformation along the fiber axis thus enhancing the orientation and alignment with much higher photoluminescence (PL) efficiency in comparison with the spin-coated films.[10]

In this article, we have synthesized three series of wholly aromatic PIs from triarylamine-based dianhydride monomers, *N,N*-bis(3,4-dicarboxyphenyl)aniline dianhydride (**3**), *N,N*-bis(3,4-dicarboxyphenyl)-1-aminonaphthalene dianhydride (**3′**), *N,N*-bis(3,4-dicarboxyphenyl)-1-aminopyrene dianhydride (**3″**),

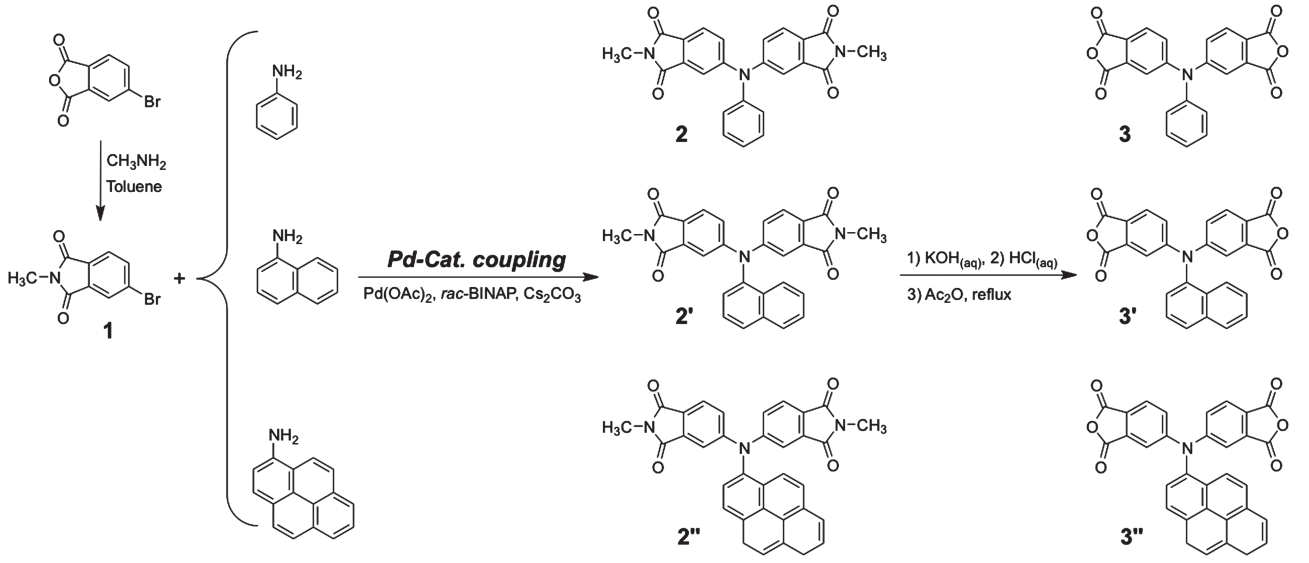

Scheme 1. Synthetic route to triarylamine-based dianhydride monomers.

with various pendant fluorophores. The incorporation of triarylamine luminogens would be expected to reveal AIE behavior for developing efficient PI solid-state emitters. Furthermore, the light-emitting ES nanofiber was also prepared and investigated to demonstrate the potential as highly efficient luminescent materials for optoelectronic applications.

2. Results and Discussion

2.1. Monomer Synthesis

N-Methyl-4-bromophthalimide (**1**) was prepared from 4-bromophthalic anhydride and methylamine according to the synthetic route outlined in **Scheme 1**. The diimide compounds resulting from double *N*-arylation reactions of primary amines with compound **1** were carried out in the presence of palladium (II) acetate, *rac*-2,2′-bis(diphenylphosphino)-1,1′-binaphthyl (*rac*-BINAP), and cesium carbonate in toluene. The resulting diimide compounds were then hydrolyzed with aqueous potassium hydroxide, giving the corresponding tetracarboxylic acids, which in turn were converted to the new dianhydride monomers by chemical cyclodehydration with acetic anhydride (Scheme 1). Elemental analysis, FTIR and NMR spectroscopic techniques were used to identify structures of the intermediate diimide compounds and the target dianhydride monomers. The FTIR spectra of the synthesized diimide compounds and dianhydride monomers are summarized in Figure S1 (Supporting Information). The carbonyl groups of diimide compounds exhibited two characteristic bands at around 1765 and 1712 cm^{-1} could be attributed to C=O asymmetric and symmetric stretching, respectively. After hydrolyzed and cyclodehydrated to dianhydride monomers, the sp^3 C−H stretch characteristic absorption bands of the CH_3 group disappeared and the carbonyl groups shifted to around 1842 and 1770 cm^{-1}. Figure S2 to S6 illustrate the NMR spectra of the diimide compounds and dianhydride monomers. Assignments of each carbon and proton are assisted by the two-dimensional NMR spectra, and these spectra agree well with the proposed molecular structure. Thus, the results of all the spectroscopic and elemental analyses suggest the successful preparation of the target dianhydride monomers.

2.2. Polymer Synthesis

Three series of PIs, **I–III**, were prepared by conventional one-step high-temperature solution polymerization of dianhydride monomers with various commercially available diamines in *m*-cresol at 200 °C in the presence of isoquinoline as the catalyst shown in **Scheme 2**. Under these conditions, polymerization reactions preceeded homogenously, leading to the formation of highly viscous polymer solutions and could be precipitated into tough fiber-like forms when slowly pouring the resulting polymer solutions into methanol. The inherent viscosities of the PIs are summarized in Table S1. All the PIs having high enough molecular weights to afford transparent and tough films via solution casting (**Figure 1**a). IR and NMR spectroscopic techniques were used to identify structures of the prepared PIs, where the spectra agree well with the proposed molecular structures (Figures S7–S9).

The IR spectra of PIs exhibited characteristic imide absorption bands at around 1773 (asymmetrical C=O), 1719 (symmetrical C=O), 1375 (C–N), and 746 cm^{-1} (imide ring deformation). The structures of these PIs were also verified by NMR spectra, Figure S8 and S9 showed a typical set of ^1H NMR spectra of PIs **IIa** and **IIIa** in $CDCl_3$, rerespectively; all the peaks also could be readily assigned to the hydrogen atoms of the recurring unit.

2.3. Polymer Properties

2.3.1. Basic Characterization

The solubility properties of PIs were investigated qualitatively at 5% w/v concentration and summarized in Table S1. The

Adv. Optical Mater. **2013**,
DOI: 10.1002/adom.201300181

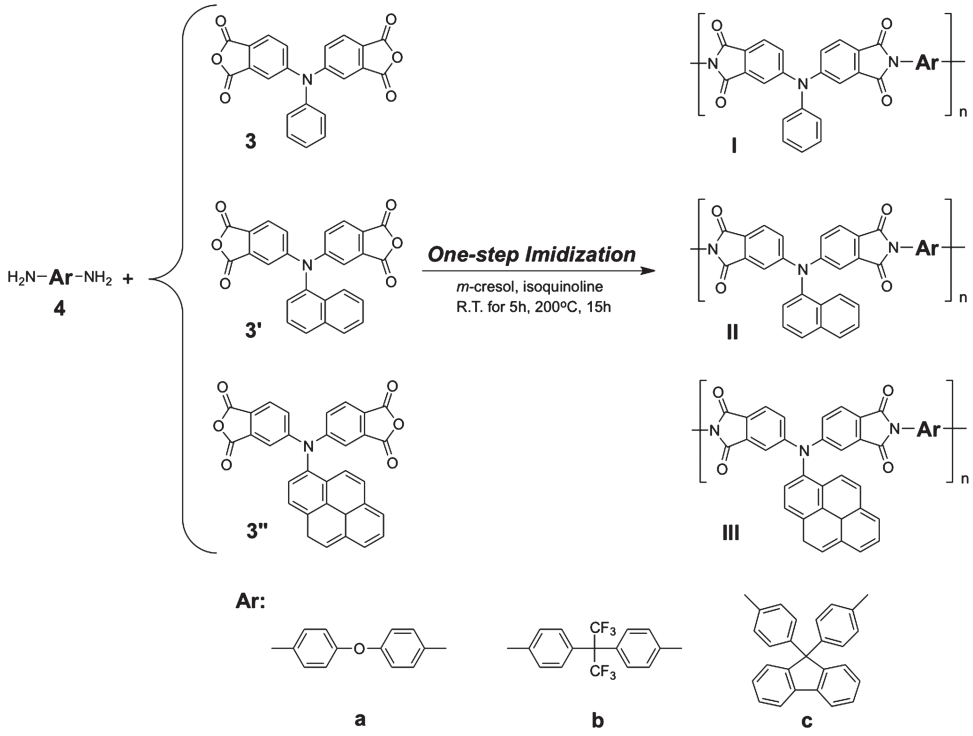

Scheme 2. Synthesis of triarylamine-based wholly aromatic PIs.

solubility behavior of these PIs depends on their chain packing and intermolecular interaction that are affected by the rigidity, symmetry, and regularity of the molecular backbone. All the PIs derived from dianhydrides with high steric hindrance and bulky pendent groups were highly soluble not only in polar aprotic organic solvents such as *N*-methyl-2-pyrrolidinone (NMP), *N,N*-dimethylacetamide (DMAc), and *m*-cresol but also in less polar solvents like $CHCl_3$. The PIs obtained from diamine **4b** revealed better solubility than those of prepared from the other diamines because of the additional contribution of the hexafluoroisopropylidene (-$C(CF_3)_2$-) fragment in the polymer backbone which reduced the intermolecular interactions. Thus, the excellent solubility makes these PIs as potential candidates for practical applications by spin-coating or inkjet-printing processes to afford high performance thin films for optoelectronic devices.

2.3.2. Thermal Properties

The thermal properties of the obtained PIs were evaluated by TGA and TMA, and the thermal behavior data are summarized in Table S2. Typical TGA curves of PIs **Ib**, **IIb**, and **IIIb** are depicted in Figure S10. All the prepared PIs exhibited good thermal stability with insignificant weight loss up to 550 °C under nitrogen or air atmosphere, and the carbonized residue (char yield) of these PIs in a nitrogen atmosphere was more than 62% at 800 °C. The high char yields of these PIs can be ascribed to their high aromatic content. The glass-transition temperatures (T_g) could be easily measured in the TMA thermograms (as shown in Figure S11); they were observed in the range of 295–420 °C, depending upon the stiffness of the polymer chain, and the higher T_g of PIs **III** could be attributed to the more chain stiffness resulting from the strong π–π interaction of pyrene group.

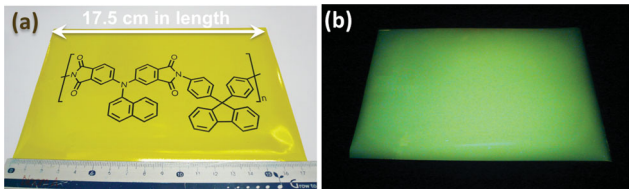

Figure 1. (a) The photograph of self-standing and flexible **IIc** film with ca. 35 µm thickness. (b) The PL photograph of **IIc** was taken under illumination of a 365 nm UV light.

2.3.3. Optical Properties

The optical properties of the diimide compounds and PIs were investigated by UV–vis and photoluminescence (PL) spectroscopy, which are summarized in Table S3 and **Table 1**, respectively. The diimide compounds showed double absorbance at around 265–269 and 378–403 nm, which exhibited PL emission maximum at 420–548 nm in NMP solution (Conc.: 10 µM) with PL qauantum yield (Φ_{PL}) ranging from 0.6% to 10.8%. The lower Φ_{PL} of diimide **2** and **2′** in the dilute solution were attributed to the intramolecular rotational relaxation thus decreasing the energy. On the contract, diimide **2″** with pendant pyrene chromophore revealed a higher Φ_{PL} (Figure S12).

In polymer system, these soluble PIs exhibited maximum UV-vis absorption bands at around 258 and 309–412 nm in NMP solution due to the π–π^* transitions of the triarylamine chromophores. **Figure 2** depicts UV-vis absorption and PL

Table 1. Optical Properties of Polyimides.

Polymer	NMP (10 μM) solution, RT			Film, RT			
	λ_{max}^{abs} [nm]	λ_{max}^{em} [nm][a)]	Φ_{PL} [%][b)]	λ_{max}^{abs} [nm]	λ_{onset}^{abs} [nm]	λ_{max}^{em} [nm][a)]	Φ_{PL} [%][c)]
Ia	(258), 407	(331), 547	(0.01), 0.7	(261), 414	472	(314), 535	(0.5), 7.6
Ib	(258), 407	(332), 556	(–)[d)], 0.8	(259), 410	468	(312), 540	(0.8), 14.2
Ic	(258), 409	(330), 547	(–)[d)], 1.2	(261), 413	468	(314), 531	(0.5), 15.2
IIa	(262), 402	(330), 530	(0.01), 0.5	(259), 407	468	(312), 526	(0.7), 8.5
IIb	(258), 401	(341), 540	(0.01), 0.6	(253), 402	457	(311), 530	(2.6), 17.9
IIc	(259), 403	(324), 534	(0.01), 0.6	(260), 404	457	(313), 521	(0.6), 22.2
IIIa	(259), 330	(330), 468	(–)[d)], 0.3	(272), 342	476	(318), 550	(0.2), 6.0
IIIb	(259), 331	(326), 470	(–)[d)], 0.3	(265), 350	470	(317), 548	(0.3), 5.8
IIIc	(258), 309	(332), 480	(–)[d)], 0.3	(274), 344	473	(319), 545	(0.2), 11.3

[a)]They were excited at λ_{max}^{abs} for solution and film states. Data shown in parentheses are those measured at relative λ_{max}^{abs}; [b)]The quantum yield was measured by using quinine sulfate (dissolved in 1 N H_2SO_4 with a concentration of 10 μM, assuming photoluminescence quantum efficiency of 0.546) as a standard at 24–25 °C; [c)]PL quantum yields of polymer thin films determined using a calibrated integrating sphere; [d)]The quatuam yield is lower than 0.01%.

behavior of PIs **Ic**, **IIc**, and **IIIc**. In the case of NMP solutions (Conc.: 10 μM), the PIs exhibited yellowish-green PL emission with Φ_{PL} ranging from 0.3 to 1.2% at the maximum peaks around 468–556 nm. Interestingly, much higher PL emission and hypsochromic shift relative to those of the solutions could be observed in solid film state (as shown in Figure 3b

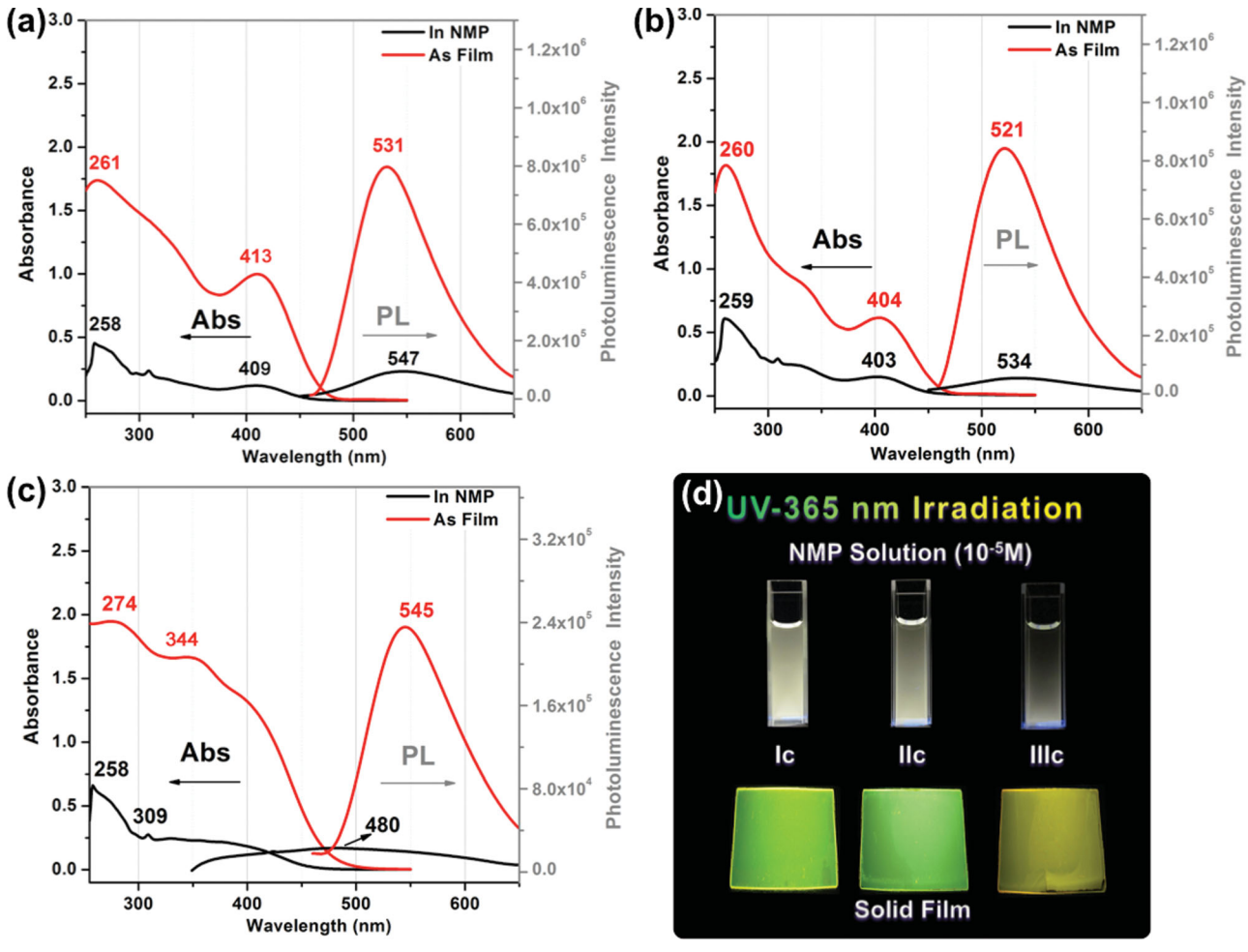

Figure 2. Absorption and photoluminescence (PL) spectra of polyimide (a) **Ic**, (b) **IIc**, and (c) **IIIc** in film and solution states. (d) Photographs were taken under illumination of a 365 nm UV light.

Adv. Optical Mater. **2013**,
DOI: 10.1002/adom.201300181

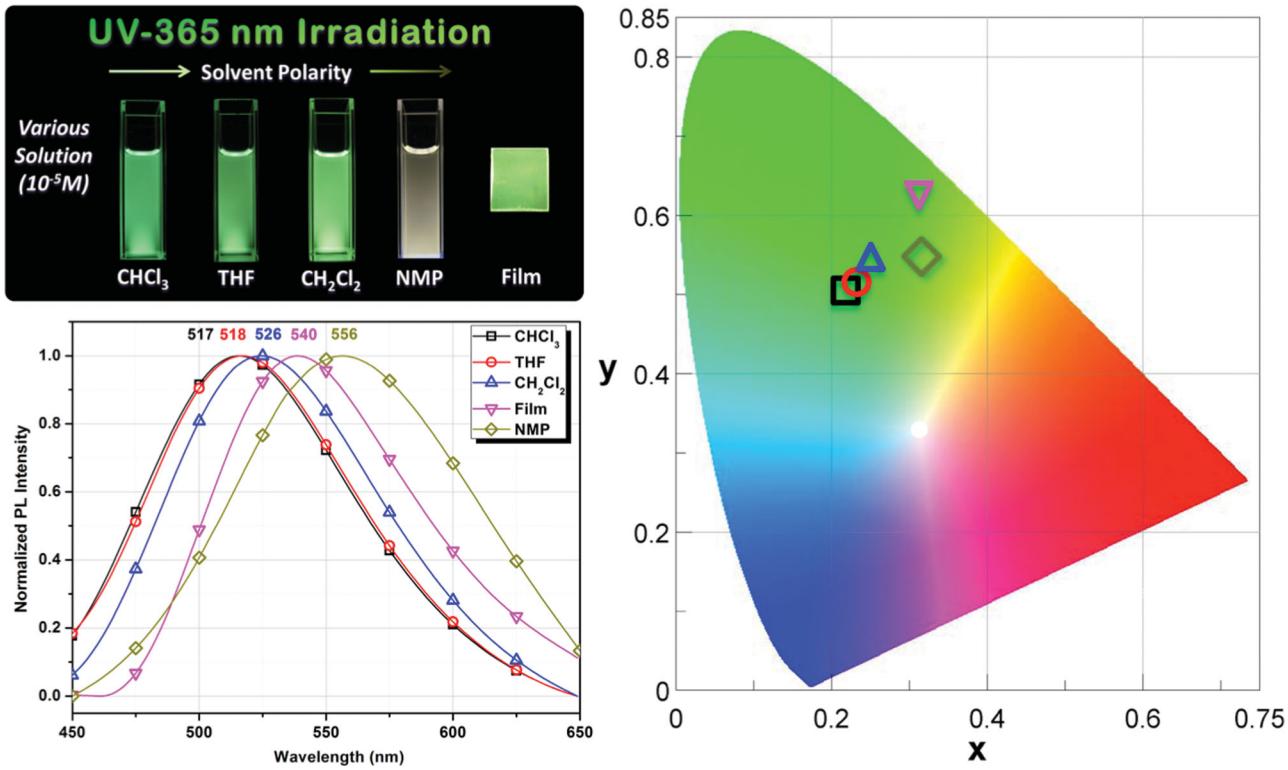

Figure 3. PL spectra of PI **Ib** in different solvents (solution concentration is 10 μM and excited with abs max). Photographs were taken under illumination of a 365 nm UV light.

and 4d). Moreover, the Φ_{PL} of the PI **IIc** film could be greatly enhanced to 22.2% estimated by integrating sphere. To the best of our knowledge, this is a notable result that PI **IIc** reveals the highest Φ_{PL} in the solid state comparing with other fluorecsent wholly aromatic PIs.[6] The phenomenon could be attributed to the solvatochromic and AIE effects resulted from the introduction of the triarylamine luminogens. On the other hand, the only slight enhancement of Φ_{PL} from solution to film state for PIs **III** would be attributed to the competition of ACQ (pyrene group) and AIE (triarylamine moiety) effects.

In order to demonstrate the solvatochromism, the optical absorption and PL of PI **Ib** and diimide compound **2** were investigated in solvents (Conc.: 10^{-5} mol/L) with different polarity. **Figure 3** and Figure S13 show the normalized PL spectra of PI **Ib** and diimide compound **2** in various solvents together with fluorescence images, and the data are summarized in **Table 2** and Table S4, respectively. These results clearly indicate that solvent polarity exerts little effect on its ground-state electronic transition, while the PL emission behavior shows strong solvent polarity dependence, resulting in the broad emission band and remarkable bathochromic shift with increasing of the solvent polarity. For diimide compound **2**, the emission color changes from blue (CIE 1931: *x*, 0.1436; *y*, 0.2235) in toluene (λ_{em} = 474 nm) to yellowish-green (CIE 1931: *x*, 0.3173; *y*, 0.5046) in DMSO (λ_{em} = 559 nm), and a lower Φ_{PL} was also observed in the solvent of higher polarity. The solvatochromism could be attributed to the fast interconversion process from the emissive local excited state to the low emissive state. Therefore,

Table 2. Photophysical Properties of Polyimide **Ib** in Different Solvents.

Solvent	ε[a)]	λ_{max}^{abs} [nm]	λ_{max}^{em} [nm][b)]	Φ_{PL} [%][c)]	CIE1931 coordinates	
					x	y
$CHCl_3$	4.8	409	517	27.8	0.2286	0.5093
THF	7.6	398	518	26.4	0.2322	0.5132
CH_2Cl_2	8.9	408	526	15.6	0.2568	0.5452
NMP	32.0	407	556	0.8	0.3253	0.5463
Film	–	410	540	14.2	0.3152	0.6253

[a)]Dielectic constant of the solvents; [b)]They were excited at λ_{max}^{abs} for solution states; [c)]The quantum yield was measured by using quinine sulfate (dissolved in 1 N H_2SO_4 with a concentration of 10 μM, assuming photoluminescence quantum efficiency of 0.546) as a standard at 24–25 °C.

Table 3. Optical Properties of polyimide **Ia** in NMP-CH_3OH with different methanol fraction [f_w; 10 μM]

f_w [vol%][a)]	λ_{max}^{abs} [nm]	λ_{max}^{em} [nm]	Φ_{PL} [%]	CIE 1931 coordinates	
				x	y
0	407	547	0.7	0.2927	0.5014
30	406	537	0.9	0.2969	0.5835
50	414	539	1.8	0.3042	0.6032
70	416	543	4.4	0.3118	0.6085
Film	414	535	7.6	0.3078	0.6332

[a)]Polymer concentration of 10 μM with different methanol fraction.

much stronger emission in the nonpolar solvents or solid state could be achieved due to the restricted molecular transitions of these diimides and their corresponding wholly aromatic polyimides.[11]

2.3.4. Aggregation-Induced Emission Enhancement (AIEE)

On the other hand, the drastically enhanced Φ_{PL} of the solid films implies that the triarylamine derivatives have inherited the AIE features. To further confirm the AIE attribution, PL spectra of the PIs **Ia** and **IIa** in NMP-methanol diluted mixtures were studied with different methanol fractions, and the results are summarized in **Table 3** and Table S5, respectively. Since the PI was insoluble in methanol but soluble in NMP, therefore by increasing the methanol fraction in the mixed solvent could change their existing forms from a solution in pure NMP to the aggregated luminogen particles in the mixtures, which will result in changes in their PL behavior. The PL spectra and images of **Ia** and **IIa** in NMP–methanol mixtures with different methanol contents are depicted in **Figure 4** and Figure S14, respectively. PIs in pure NMP exhibited very weak yellow PL emission with maximum peak at around 540 nm, while the PL emission was slightly blue-shifted and intensity could be enhanced with increasing the methanol fraction. The enhancement in PL intensity can be attributed to an AIE effect caused by the formation of molecular aggregates, in which the restriction of intramolecular rotations leads to increased fluorescent emission.[9] Futhermore, dynamic light scattering measurements of PI **Ia** in NMP–methanol with methanol fraction of 50 and 70 vol% (Conc.: 10 μM) shown in Figure S15 were also measured to confirm the aggregation formation of polymer after addition of large amount of methanol caused by restriction of molecular transitions. These results demonstrate that the triarylamine unit is indeed AIE-active.

2.3.5. Optical and Morphological Properties of Electrospun Fibers

The polymeric ES fiber of AIE-active **IIc** was further fabricated to investigate and confirm the phenomenon of high Φ_{PL} in solid film state. The FE-SEM images of the ES fiber revealing smooth fiber-like structure without beads formation are shown in **Figure 5**. The PL spectra of ES fiber exhibited bathochromic shift to its film state, suggesting the higher orientation and

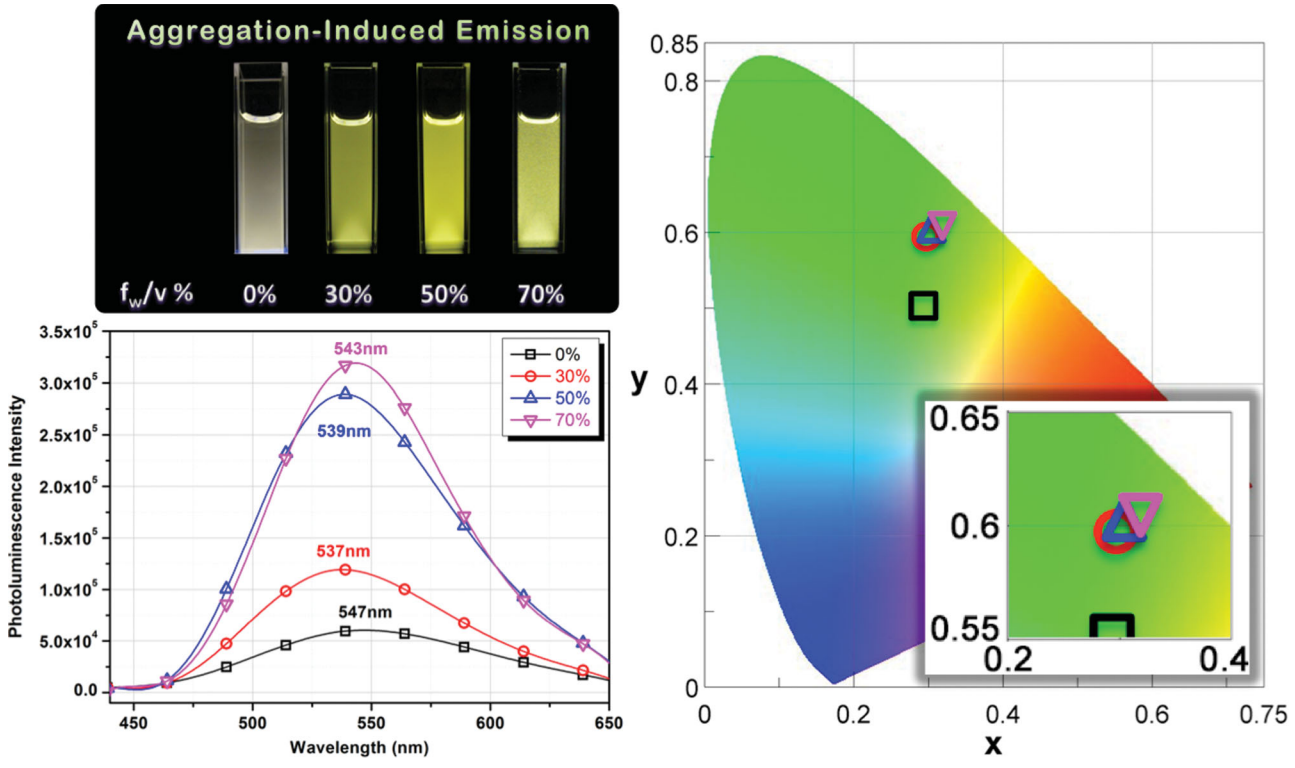

Figure 4. PL spectra of PI **Ia** in NMP–MeOH with different methanol fraction (f_w/vol%) (solution concentration is 10 μM and excited with λ_{max}). Photographs were taken under illumination of a 365 nm UV light..

DOI: 10.1002/adom.201300181

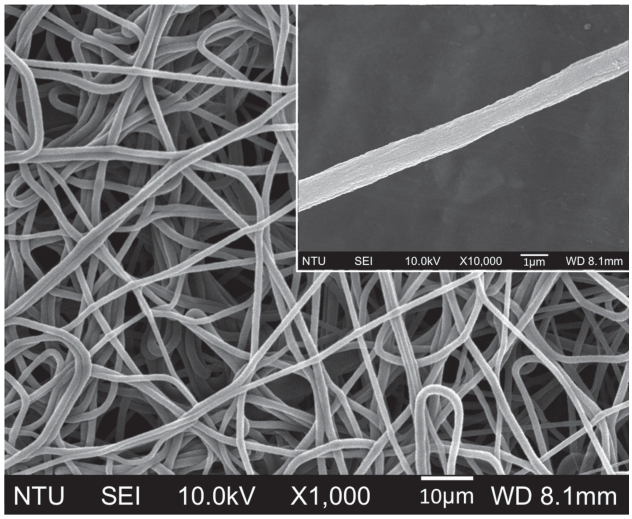

Figure 5. SEM image of ES nanofiber of PI **IIc**.

alignment of the polymer chains in the fiber state. **Figure 6** shows the optical behaviors and PL photographs of dilute solution, thin film, and ES fiber of PI **IIc**. Interestingly, the ES fiber of **IIc** exhibited notable PL emission with enhanced quantum yield up to 26.3% when compared with its solid film (as summarized in **Table 4**). The further enhancement of Φ_{PL} in fiber state implies that the judicious combination of the AIE feature and ES nanofiber fabrication is an essential approaching for obtaining the solid-state high-efficiency PL wholly aromatic functional polyimides.

3. Conclusion

Novel AIE-active triarylamine-containing wholly aromatic functional PIs were readily prepared *via* one-step imidation from newly synthesized aromatic dianhydrides, (**3'**) and (**3''**), and could be utilized to prepare the nanofiber by ES method. The SEM results exhibited that the obtained nano-structure was quite uniform without any bead in the nanofiber surface. Notably, the triarylamine-based PIs having an AIE feature are highly emissive in the solid state with Φ_{PL} up to 22%, which could be further enhanced in the form of ES nanofiber with the highest Φ_{PL} of 26% to date, demonstrating the incorporation of the triarylamine luminogen with AIE feature and ES nanofiber fabrication is an outstanding approaching to obtain the solid-state high-efficiency PL wholly aromatic functional polyimides and are desirable candidate materials for advanced optoelectronic applications.

4. Experimental Section

Materials: 1-aminopyrene[12] and *N*,*N*-bis(3,4-dicarboxyphenyl) aniline dianhydride[13] (**3**) were prepared according to the previously reported procedures. Synthetic details and characterization data of new dianhydride monomers, *N*,*N*-bis(3,4-dicarboxyphenyl)-1-aminonaphthalene dianhydride (**3'**) and *N*,*N*-bis(3,4-dicarboxyphenyl)-

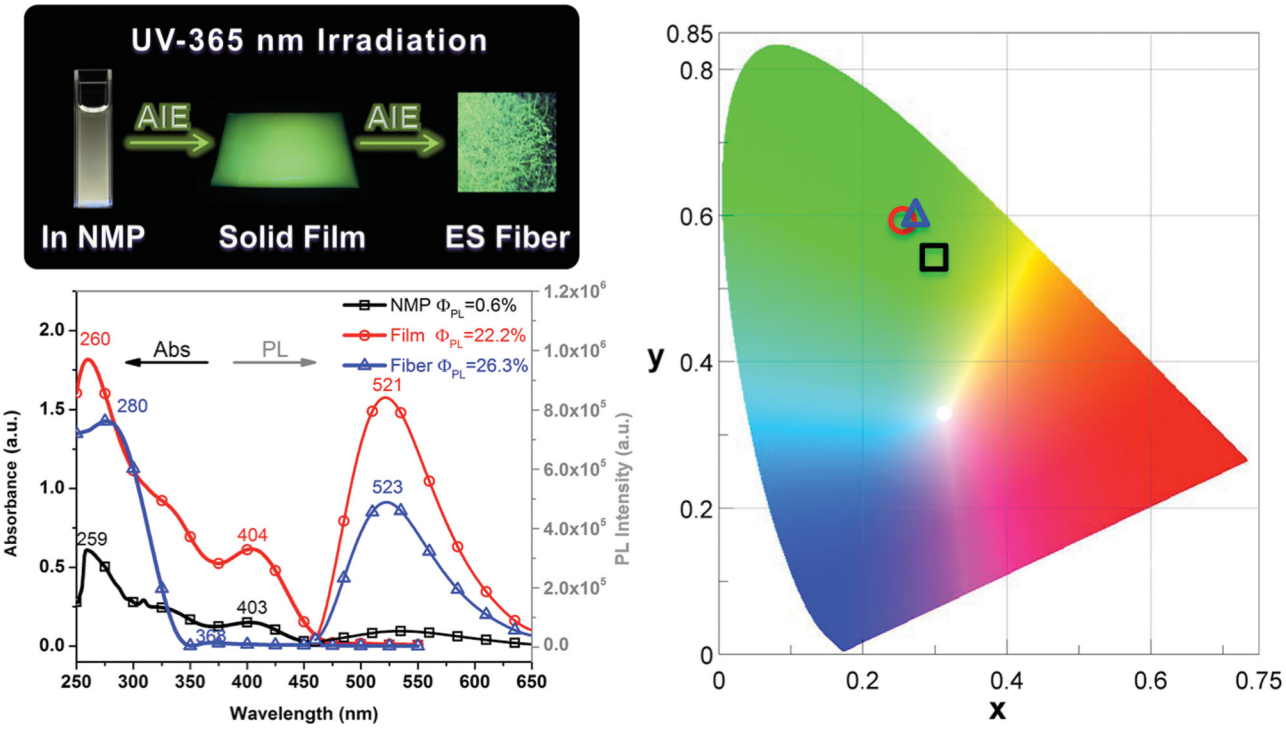

Figure 6. Absorbance and PL spectra of PI **IIc** in solution, solid film, and ES fiber states. Photographs were taken under illumination of a 365 nm UV light.

Table 4. Optical Properties of polyimide **IIc.**

	NMP (10 μM) solution	Solid film	ES fiber
λ_{max} [nm]	(259), 403	(260), 404	(280), 368
λ_{em} [nm][a)]	(324), 534	(313), 521	(317), 523
Φ_{PL} [%][b,c)]	(0.01), 0.6	(0.6), 22.2	(0.3), 26.3
CIE 1931 coordinates (x,y)	(0.2880, 0.5406)	(0.2486, 0.5958)	(0.2698,0.5995)

[a)]They were excited at λ_{max} for solid and solution states. Data shown in parentheses are those measured at relative λ_{max} [abs]; [b)]The quantum yield in the solution state (NMP) was measured by using quinine sulfate (dissolved in 1 N H_2SO_4 with a concentration of 10 μM, assuming photoluminescence quantum efficiency of 0.546) as a standard at 24–25 °C; [c)]PL quantum yields in solid states (film and fiber) were determined using a calibrated integrating sphere.

1-aminopyrene dianhydride (**3″**), are included in the Supporting Information. Commercially available 4,4'-oxydianiline (**4a**), 2,2-bis(4-aminophenyl)hexafluoropropane (**4b**), and 2,3,5,6-tetramethylbenzene-1,4-diamine (**4d**) were purified by vacuum sublimation. 9,9-Bis(4-aminophenyl)fluorene (**4c**) was recrystallized by ethanol in a nitrogen atmosphere and then dried in vacuo prior to use. All other reagents were used as received from commercial sources.

Synthesis of Polyimides by One-Step Method: The synthesis of PI **IIa** was used as an example to illustrate the general synthetic route used to produce the PIs. Into a 50 mL round-bottom flask were added 0.20 g (1.00 mmol) of diamine **4a**, 0.43 g (1.00 mmol) of dianhydride **3′**, 0.24 mL isoquinoline and 6.0 mL *m*-cresol. The reaction mixture was stirred at room temperature in nitrogen atmosphere for 5 h. Then, the reaction temperature was increased to 200 °C for 15 h. After the imidization reaction, the mixture was cooled to room temperature, the viscous polymer solution was then poured slowly into 300 mL of stirred methanol giving rise to a brownish fibrous precipitate that was collected by filtration, washed thoroughly with methanol, and dried at 70 °C for 15 h. Reprecipitation of the polymer by DMAc/methanol was carried out twice for further purification. The inherent viscosity of obtained polyimide **IIa** was 0.42 dL/g (measured at a concentration of 0.5 g/dL in DMAc at 30 °C). The FT-IR spectrum of **IIa** (film) exhibited characteristic imide absorption bands at around 1774 (asymmetrical C = O), 1719 (symmetrical C = O), 1371 (C-N), and 746 cm^{-1} (imide ring deformation). ^{1}H NMR ($CDCl_3$, δ, ppm): 7.95. (t, 2H, H_c + H_d), 7.78 (d, 2H, H_i), 7.75 (d, 1H, H_g), 7.55 (m, 4H, H_h + H_a + H_b), 7.41 (m, 4H, H_e + H_f + H_j), 7.35 (d, 2H, H_l), and 7.13 (d, 2H, H_k).

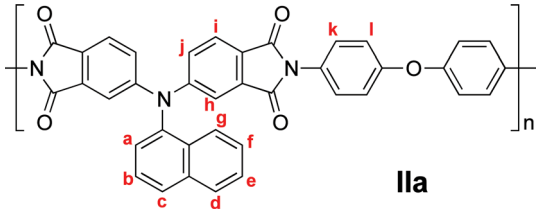

IIa

Preparation of the Polyimide Films: A solution of the polymer was made by dissolving about 1.2 g of the PI sample in 20 mL of DMAc. The homogeneous solution was poured onto a glass substrate (18 cm × 12 cm), which was heated in oven at 70 °C for 6 h to remove most of the solvent, then the semi-dried film was further dried in vacuo at 160 °C for 10 h. The obtained films were about 35 μm thick and were used for solubility tests and thermal analyses.

Fabrication of Electrospun Fibers: The polymer solution of PI **IIc** with the concentration of 25 wt% in DMAc was used to produce the electrospun (ES) fiber. The ES fiber was prepared using a single-capillary spinneret. First, the solution was fed into the syringe pumps (KD Scientific model 100) connected to the metallic needle, with the feed rate of 0.1 mL/h. The metallic needle was connected to a high-voltage power supply (YSTC), and a piece of aluminum foil was placed 6 cm below the tip of the needle to collect the nanofiber. The spinning voltage was set at 15 kV. All experiments were carried out at room temperature.

Supporting Information

Supporting Information is available from the Wiley Online Library or from the author.

Acknowledgements

We are grateful acknowledge to the National Science Council of Taiwan for the financial support. Supporting Information is available online from Wiley InterScience or from the author.

Received: April 24, 2013
Revised: June 9, 2013
Published online:

[1] C. E. Sroog, *J. Polym. Sci. Macromol. Rev.* **1976**, *11*, 161.
[2] G. S. Liou, H. J. Yen, in Polymer Science: A Comprehensive Reference, Vol 5 (Eds: K. Matyjaszewski, M. Möller), Elsevier BV, Amsterdam **2012**, pp.497–535.
[3] a) H. Ishida, S. T. Wellinghoff, E. Baer, J. L. Koenig, *Macromolecules* **1980**, *13*, 826; b) D. Erskine, P. Y. Yu, S. C. Freimanis, *J. Polym. Sci., Part C: Polym. Lett.* **1988**, *26*, 465; c) M. Hasegawa, M. Kochi, I. Mita, R. Yokota, *J. Polym. Sci., Part C: Polym. Lett.* **1989**, *27*, 263; d) M. Hasegawa, I. Mita, M. Kochi, R. Yokota, *Eur. Polym. J.* **1989**, *25*, 349; e) Q. Jin, T. Yamashita, K. Horie, R. Yokota, I. Mita, *J. Polym. Sci., Part A: Polym. Chem.* **1993**, *31*, 2345; f) Q. Li, K. Horie, R. Yokota, *J. Photopolym. Sci. Technol.* **1997**, *10*, 49; g) S. A. Lee, T. Yamashita, K. Horie, *J. Polym. Sci., Part B: Polym. Phys.* **1998**, *36*, 1433; h) M. Hasegawa, K. Horie, *Prog. Polym. Sci.* **2001**, *26*, 259; i) M. Sato, Y. Nakamoto, K. Yonetake, J. Kido, *Polym. J.* **2002**, *34*, 601; j) M. Hasegawa, M. Koyanaka, *High Perform. Polym.* **2003**, *15*, 47.
[4] S. Ando, T. Matsuura, S. Sasaki, *Polym. J.* **1997**, *29*, 69.
[5] a) R. Dien-Hart, W. W. Wright, *Macromol. Chem.* **1971**, *143*, 189; b) M. Hasegawa, Y. Shindo, T. Sugimura, S. Ohshima, K. Horie, M. Kochi, R. Yokota, I. Mita, *J. Polym. Sci., Part B: Polym. Phys.* **1993**, *31*, 1617.
[6] a) H. Ghassemi, J. H. Zhu, *J. Polym. Sci., Part B: Polym. Phys.* **1995**, *33*, 1633; b) S. Fomine, M. Marin, L. Fomina, R. Salcedo, E. Sansores, J. M. Medez, C. F. Jimenez, T. Ogawa, *Polym. J.* **1996**, *28*, 641; c) S. Fomine, C. Sa`nchez, L. Fomina, J. C. Alonso, T. Ogawa, *Macromol. Chem. Phys.* **1996**, *197*, 3667; d) S. M. Pyo, S. I. Kim, T. J. Shin, M. Ree, K. H. Park, J. S. Kang, *Polymer* **1999**, *40*, 125; e) M. Ree, S. I. Kim, S. M. Pyo, T. J. Shin, H. K. Park, J. C. Jung, *Macromol. Symp.* **1999**, *142*, 73; f) H. K. Park, M. Ree, *Synth. Met.* **2001**, *117*, 197; g) W. Huang, D. Yan, Q. Lu, *Polym. Bull.* **2003**, *49*, 417; h) S. Xu, M. Yang, J. Wang, H. Ye, X. Liu, *Synth. Met.* **2003**,

132, 145; i) S. C. Hsu, W. T. Whang, S. C. Chen, *J. Polym. Res.* **2003**, *10*, 7.

[7] a) T. P. I. Saragi, T. Spehr, A. Siebert, T. Fuhrmann-Lieker, J. Salbeck, *Chem. Rev.* **2007**, *107*, 1011; b) A. C. Grimsdale, K. L. Chan, R. E. Martin, P. G. Jokisz, A. B. Holmes, *Chem. Rev.* **2009**, *109*, 897; c) J. Liu, J. W. Y. Lam, B. Z. Tang, *Chem. Rev.* **2009**, *109*, 5799.

[8] a) G. S. Liou, S. H. Hsiao, H. W. Chen, *J. Mater. Chem.* **2006**, *16*, 1831; b) J. Wakita, H. Sekino, K. Sakai, Y. Urano, S. Ando, *J. Phys. Chem. B* **2009**, *113*, 15212; c) Y. C. Kung, W. F. Lee, S. H. Hsiao, G. S. Liou, *J. Polym. Sci., Part A: Polym. Chem.* **2011**, *49*, 2210; d) H. J. Yen, C. J. Chen, G. S. Liou, *Chem. Commun.* **2013**, *49*, 630.

[9] a) Y. Hong, J. W. Y. Lam, B. Z. Tang, *Chem. Commun.* **2009**, 4332; b) M. Wang, X. Pan, X. Q. Fang, L. Guo, W. Q. Liu, C. N. Zhang, Y. Huang, L. H. Hu, S. Y. Dai, *Adv. Mater.* **2010**, *22*, 5526; c) H. Wang, F. Li, I. Ravia, B. R. Gao, Y. P. Li, V. Medvedev, H. B. Sun, N. Tessler, Y. G. Ma, *Adv. Funct. Mater.* **2011**, *21*, 3770.

[10] a) C. C. Kuo, C. H. Lin, W. C. Chen, *Macromolecules* **2007**, *40*, 6959; b) S. Chuangchote, T. Sagawa, S. Yoshikawa, *J. Appl. Phys.* **2008**, *47*, 787; c) L. Xu, H. W. Song, B. A. Dong, Y. Wang, X. Bai, G. L. Wang, Q. Liu, *J. Phys. Chem. C* **2009**, *113*, 9609; d) H. C. Chen, C. T. Wang, C. L. Liu, Y. C. Liu, W. C. Chen, *J. Polym. Sci. Part B: Polym. Phys.* **2009**, *47*, 463.

[11] a) A. Qin, J. W. Y. Lam, B. Z. Tang, *Prog. Polym. Sci.* **2012**, *37*, 182; b) Y. N. Hong, J. W. Y. Lam, B. Z. Tang, *Chem. Soc. Rev.* **2011**, *40*, 5361; c) W. Z. Yuan, Y. Y. Gong, S. M. Chen, X. Y. Shen, J. W. Y. Lam, P. Lu, Y. W. Lu, Z. M. Wan, R. R. Hu, N. Xie, H. S. Kwok, Y. M. Zhang, J. Z. Sun, B. Z. Tang, *Chem. Mater.* **2012**, *24*, 1518.

[12] Y. C. Kung, S. H. Hsiao, *J. Mater. Chem.* **2010**, *20*, 5481.

[13] W. Li, S. Li, Q. Zhang, S. Zhang, *Macromolecules* **2007**, *40*, 8205.